*MOLECULAR PLANT PATHOLOGY* (2009) **10**(3), 389–401 DOI: 10.1111/J.1364-3703.2009.00539.X

# Characterization of a putative endoxylanase in the migratory plant-parasitic nematode *Radopholus similis*

ANNELIES HAEGEMAN[1], BARTEL VANHOLME[2] AND GODELIEVE GHEYSEN[1]*

[1]*Faculty of Bioscience Engineering (FBE), Department of Molecular Biotechnology, Ghent University, Coupure links 653, B-9000 Ghent, Belgium*
[2]*Department of Plant Systems Biology, Flanders Institute for Biotechnology (VIB), Ghent University, Technologiepark 927, B-9052 Ghent, Belgium*

## SUMMARY

Plant-parasitic nematodes have developed an arsenal of enzymes to degrade the rigid plant cell wall. In this article, we report the presence of a putative endoxylanase in the migratory endoparasitic nematode *Radopholus similis*. This enzyme is thought to facilitate the migration of the nematode, as it breaks down xylan, the major component of hemicellulose. The corresponding gene (*Rs-xyl1*) was cloned and the sequence revealed three small introns. Interestingly, the position of all three introns was conserved in a putative endoxylanase from *Meloidogyne hapla*, and the position of one intron was conserved in two endoxylanases from *Meloidogyne incognita*, which suggests a common ancestral gene. The spatial and temporal expression of the *Rs-xyl1* gene was examined by *in situ* hybridization and semi-quantitative reverse transcriptase-polymerase chain reaction. The putative protein consists of a signal peptide, a catalytic domain and a carbohydrate-binding module (CBM). The catalytic domain showed similarity to both glycosyl hydrolase family 5 (GHF5) and GHF30 enzymes. Using Hidden Markov Model profiles and phylogenetic analysis, we were able to show that Rs-XYL1 and its closest homologues are not members of GHF5, as suggested previously, but rather form a subclass within GHF30. Silencing the putative endoxylanase by double-stranded RNA targeting of the CBM region resulted in an average decrease in infection of 60%, indicating that the gene is important for the nematode to complete its life cycle.

## INTRODUCTION

During evolution, nematodes adapted to a wide range of environmental conditions. A subset of nematode species evolved into effective plant parasites with various life styles. They all developed a stylet, a hollow needle-like structure that is used to withdraw the contents of plant cells on which they feed. In addition to a role in feeding, the stylet is used to mechanically damage the rigid cell wall, as well as to inject enzymes into the plant tissue to weaken the plant cell wall during migration. These cell wall-degrading enzymes are produced in large pharyngeal glands located in the anterior half of the nematode's body. The most extensively studied nematode cell wall-degrading enzymes, endo-1,4-β-glucanases, have been identified in both sedentary (Rosso *et al.*, 1999; Smant *et al.*, 1998) and migratory (Haegeman *et al.*, 2008; Kikuchi *et al.*, 2004; Uehara *et al.*, 2001) species. Several other cell wall-degrading enzymes have been identified, such as pectate lyase (de Boer *et al.*, 2002; Doyle and Lambert, 2002; Kikuchi *et al.*, 2006; Vanholme *et al.*, 2007), polygalacturonase (Jaubert *et al.*, 2002) and recently a xylanase (Mitreva-Dautova *et al.*, 2006). The latter enzymes have only been found in sedentary nematodes, with the exception of pectate lyase, which was also identified in the migratory nematode *Bursaphelenchus xylophilus* (Kikuchi *et al.*, 2006).

Xylan is composed of β-1,4-linked xylopyranose units and can have various substituents and variable structures according to the plant species (Collins *et al.*, 2005). It is the major component of hemicellulose, a complex of polymeric carbohydrates in plant cell walls, and, next to cellulose, the second most abundant polysaccharide in nature. Xylan is found at the interface between lignin and cellulose, where it plays a role in fibre cohesion and plant cell wall integrity. In monocotyledons, it is located in the primary cell wall, whereas, in dicotyledons, it is the major constituent of the secondary cell wall. Endo-1,4-β-xylanases (EC 3.2.1.8) depolymerize the non-hydrolysed xylan polymer by the random cleavage of the xylan backbone (Subramaniyan and Prema, 2002). These enzymes are mainly produced by plant pathogenic bacteria and fungi, as well as by endosymbionts located in the digestive tracts of various wood-boring insects (Brennan *et al.*, 2004). Glycosyl hydrolases are classified into different families according to their sequence similarity (Henrissat and Bairoch, 1996). Endo-1,4-β-xylanases are mostly classified in glycosyl hydrolase families 10 and 11 (GHF10 and GHF11), but some have also been designated to GHF5, GHF7, GHF8, GHF16, GHF26, GHF43, GHF51 and GHF62 (Collins *et al.*, 2005) (Carbohydrate Active Enzymes website http://www.cazy.org) (Coutinho

* *Correspondence*: Tel.: +003292645888; Fax: +003292646219;
E-mail: Godelieve.Gheysen@UGent.be

and Henrissat, 1999). To our knowledge, only three endoxylanases have been found in animals: one in Gastropoda (*Ampullaria crossean* AAY46801, GHF10), one in Insecta (*Phaedon cochleariae* CAA76932, GHF11) and one in Nematoda (*Meloidogyne incognita* AAF37276, GHF5). The nematode endoxylanase, Mi-XYL1, has similarity to a range of bacterial endoxylanases. Most of these have been designated as GHF5, although there is some confusion about this classification as the proteins also show similarity to GHF30 enzymes. Originally, the first enzyme of this group was classified into a new family located between GHF5 and GHF30 (Keen *et al.*, 1996). Other authors also suggested that they should be classified into a new family (Hurlbert and Preston, 2001; Suzuki *et al.*, 1997). However, since the first crystallographic structure of one of these xylanases was unravelled, they have been inconsistently classified as GHF5 (John *et al.*, 2006; Larson *et al.*, 2003; Mitreva-Dautova *et al.*, 2006).

*Radopholus similis*, or the burrowing nematode, is a (sub)tropical migratory endoparasitic nematode which belongs to the family Pratylenchidae. It has many different host plants, both dicotyledons and monocotyledons, with banana being the most economically important crop. *Radopholus similis* infection causes bad anchorage of the banana root system as a result of necrosis of the root cortex, which can lead to severe toppling (Fogain, 2000). Juveniles sometimes feed ectoparasitically on plant root hairs, whereas adults generally feed and migrate within the root tissue. As opposed to females, adult males do not feed and have a degenerate stylet and reduced pharyngeal glands, questioning their parasitic status (Duncan and Moens, 2006; Trinh *et al.*, 2004). Only recently, some molecular information has become available about this widespread and economically important nematode species. The first described cell wall-degrading enzymes of *R. similis* were four different endo-1,4-β-glucanases (Haegeman *et al.*, 2008). A recent expressed sequence tag (EST) study revealed some other interesting genes, including an EST with homology to an endo-1,4-β-xylanase (Jacob *et al.*, 2008). In this study, we report the further characterization of the corresponding gene. It is the first putative endoxylanase in a migratory plant-parasitic nematode; moreover, it is the first characterized animal endoxylanase that includes a putative carbohydrate-binding module (CBM).

## RESULTS

### Putative endoxylanases in *R. similis* and *Meloidogyne* species

The xylan activity assay on nematode homogenate from *R. similis* showed a clear halo, which was not present in the negative control, indicating that *R. similis* contains active enzymes that are able to break down xylan (Fig. 1). Screening over 7000 ESTs of *R. similis* revealed a tag of 521 bp with homology to an endoxylanase of *Aeromonas punctata* (BLASTX *E*-value = 2e−34) (Jacob

**Fig. 1** Xylan activity assay. Left: nematode homogenate of *Radopholus similis*; right: negative control.

*et al.*, 2008). Based on this sequence, primers were constructed to clone both the genomic (1337 bp) and coding (1203 bp) sequences of the corresponding gene. The gene was named *Rs-xyl1* and was submitted to the GENBANK database (EU190885). Comparing the genomic DNA with the cDNA revealed three short introns (43, 44 and 47 bp). The first two introns, in phases 2 and 0, respectively, contain the consensus GT/AG splice site (Blumenthal and Steward, 1997), whereas the third intron (phase 0) has the alternative splice site GC/AG. The coding sequence has an overall GC percentage of 61%, with GC1 and GC2 each 49% and GC3 85%. The introns have a GC percentage of 60%.

Nematode endoxylanases have been described previously only for the sedentary nematode *M. incognita* (Mitreva-Dautova *et al.*, 2006) and, in the recently published genome of *M. incognita*, six endoxylanases were identified (Abad *et al.*, 2008). As, to date, only coding sequences are publicly available for these genes and we were interested in the number and specific position of introns, primers were constructed to isolate the corresponding genomic clones. Two genomic fragments of 1503 and 1357 bp were amplified from *M. incognita*, and were named *Mi-xyl2* (EU475875) and *Mi-xyl3* (EU475876), respectively. Their deduced coding sequences showed minor differences to the original cDNA sequence of *Mi-xyl1* as presented by Mitreva-Dautova *et al.* (2006) (8 bp in the case of *Mi-xyl2* and 15 bp in the case of *Mi-xyl3*). These isolated genomic sequences are probably other copies of the gene in the genome, or allelic variants. Both genomic sequences contain a single intron in phase 0, holding the canonical GT/AG donor/acceptor motif. The intron of *Mi-xyl2* is 642 bp, whereas that of *Mi-xyl3* is shorter (496 bp). The introns only show similarity at the extensions: approximately 80 nucleotides at the 5′ end of the introns and 120 nucleotides at the 3′ end. Interestingly, both introns were located at the same position as the second intron of *Rs-xyl1*.

A TBLASTN with Rs-XYL1 against the genome of *Meloidogyne hapla* revealed one contig (contig 2188) with significant similarity (*E*-value = 4e−24). This putative endoxylanase of *M. hapla* includes the putative CBM and contains three predicted introns of 148, 214 and 275 bp, all with a GT/AG splice site. The introns

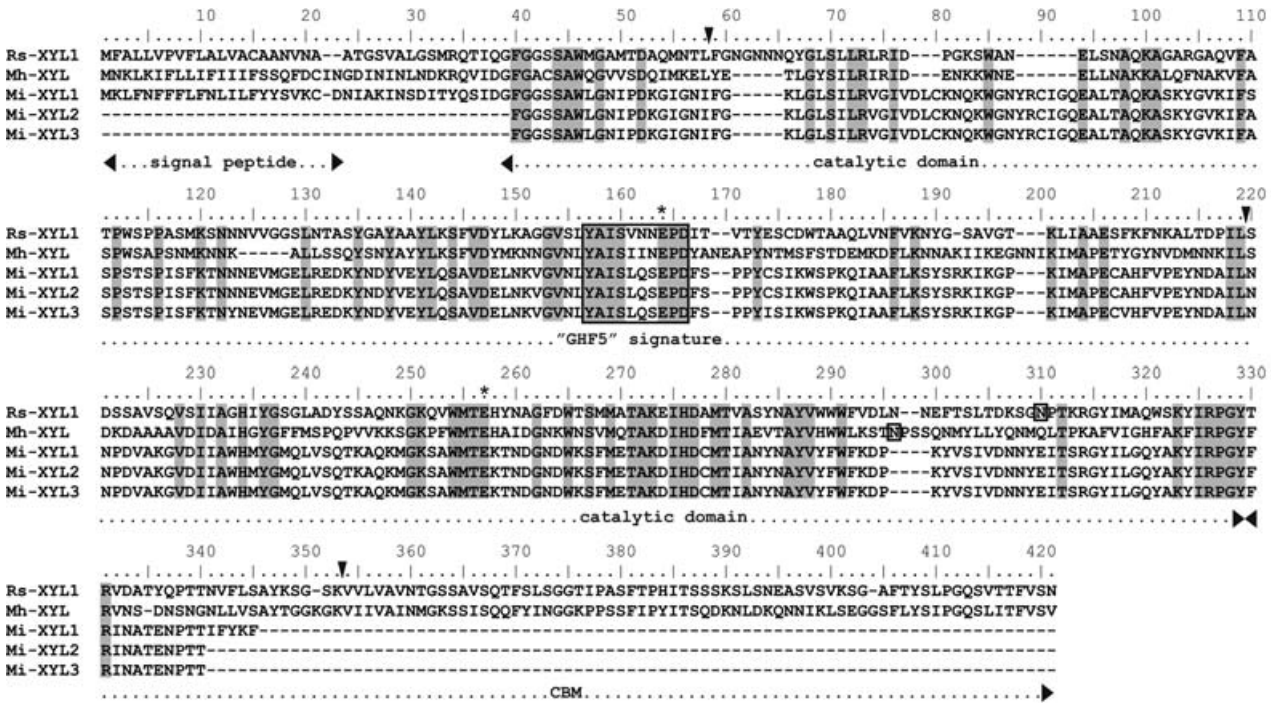


**Fig. 2** Alignment of Rs-XYL1 with Mi-XYL1, the isolated sequences Mi-XYL2 and Mi-XYL3 and the putative Mh-XYL. The locations of the signal peptide, catalytic domain, the putative glycosyl hydrolase family 5 (GHF5) signature and the putative carbohydrate-binding module (CBM) are indicated. Stars indicate the two catalytic residues. The three arrows indicate the positions of the introns in Rs-XYL1 and Mh-XYL. Possible *N*-glycosylation sites are boxed. The threshold for shading is 100%.

are located at exactly the same positions as the three introns from *Rs-xyl1*.

## Protein properties and structure

The putative protein sequence of 400 amino acids, called Rs-XYL1, contains a putative 21-amino-acid signal peptide for secretion. The predicted molecular mass of the mature endoxylanase is 40 kDa. NetNGlyc predictions revealed one putative *N*-glycosylation site at position 270 of the mature protein.

A search for protein domains resulted in hits for a glucosylceramidase of GHF30 (EC 3.2.1.45) (*E*-value = 3.3e−07) and, with low support, a CBM of family II (*E*-value = 3.7e+02). Alternatively, the CATH database (Pearl *et al.*, 2003) was searched, and high support was found for a glycoside hydrolase domain (*E*-value = 1.4e−68). Thus, the protein consists of an N-terminal signal peptide for secretion of 21 amino acids, and two putative modules: a glycoside hydrolase catalytic domain of 274 amino acids and a C-terminal CBM of 90 amino acids. This putative endoxylanase is the first animal xylanase found with a putative CBM.

The putative endoxylanase found in the *M. hapla* genome has a predicted signal peptide of 24 amino acids, a catalytic domain of 272 amino acids and a putative CBM of 91 amino acids. One possible *N*-glycosylation site is present. The protein sequence deduced from *Mi-xyl2* of *M. incognita* is identical to Mi-XYL1, whereas Mi-XYL3 differs in three amino acids from Mi-XYL1. An alignment of Rs-XYL1 with the endoxylanase sequences of *M. incognita* and *M. hapla* is shown in Fig. 2.

A three-dimensional model was created using a xylanase from *Erwinia chrysanthemi* as template [Protein Data Bank (PDB) identifier 1NOF] (Fig. 3). As the proteins are 45% identical and 75% similar, the simplest homology modelling scenario could be used. The α- and β-chains of the catalytic domain fold into an $(\alpha/\beta)_8$-barrel structure (indicated in green in Fig. 3), whereas eight consecutive β-strands of the CBM form a β-sandwich (indicated in yellow in Fig. 3). One β-strand at the N-terminal end of the mature protein (13 amino acids) contributes to the C-terminal β-sandwich (indicated in purple in Fig. 3).

## Database searches and phylogenetic analysis

A BLASTP search was performed using the catalytic domain as query. There were two groups of BLAST results. The first group included the top hits (*E*-value between 1e−73 and 1e−22), and consisted of 24 bacterial sequences and the nematode endoxylanases. Both the literature and CAZy website (http://www.cazy.org) classified most of these proteins as GHF5

 

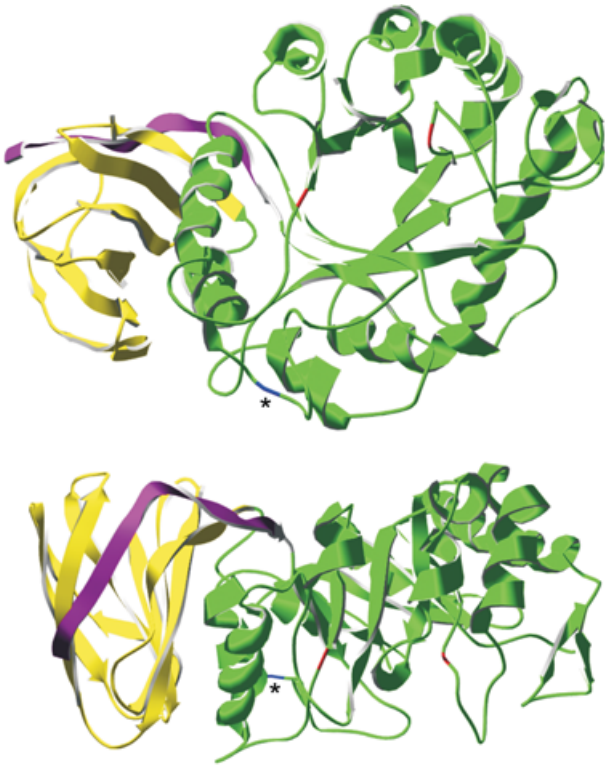

**Fig. 3** Three-dimensional model of the putative endoxylanase Rs-XYL1 from *Radopholus similis*, based on the three-dimensional model of the *Erwinia chrysanthemi* endoxylanase 1NOF (top, front view; bottom, side view). The catalytic domain is indicated in green and the carbohydrate-binding module (CBM) in yellow. The β-strand at the N-terminal end of the protein, which contributes to the CBM, is shown in purple. The catalytic residues (Glu153 and Glu240) are shown in red and the possible *N*-glycosylation site (Asn291) is indicated in blue and with a star.

enzymes, although they all showed higher similarity to GHF30 enzymes according to the Conserved Domain Database (CDD) (*E*-value < 1e−3). Similarly, HMMer searches (HMM, Hidden Markov Model), using both the GHF5 and GHF30 profiles, classified all proteins (including Rs-XYL1) as GHF30, except for Mi-XYL1. No significant matches were found when using the GHF5 profile. These observations question the classification of the proteins to the GHF5 subclass. The second group of BLAST hits, which show less homology to Rs-XYL1 (*E*-value between 1e−14 and 1e−4), appeared to be GHF30 enzymes from both bacteria and fungi, mostly named glycosyl hydrolase or glucosylceramidase. It should, however, be noted that only two of these hits are classified as GHF30 according to the CAZy database. The others have not been classified at all, although they all have a significant match to the GHF30 profile.

A phylogenetic tree, including the two groups of BLAST hits and some GHF5 enzymes, revealed a clear separation of two clusters, highly supported with a posterior probability value of 1.00 (Fig. 4). The first cluster includes the 'true' GHF5 enzymes, whereas the second cluster includes all proteins which showed homology to the catalytic domain of Rs-XYL1. From now on, we will call the first cluster the 'GHF5 cluster' and the second cluster the 'GHF30 cluster'. Within the GHF30 cluster, a first group is separated from the other proteins with high support (posterior probability of 1.00). This group consists of all fungal sequences and one bacterial sequence. The rest of the GHF30 cluster is not well resolved (posterior probability values less than 0.60). However, Rs-XYL1 and all the BLAST top hits, with very low *E*-values, form a monophyletic group. This group is not well resolved from the other BLAST hits with higher *E*-values, as the posterior probability is only 0.56. This low posterior probability is mainly a result of the protein ZP_01576533. Discarding this protein from the dataset results in a monophyletic cluster of all other top BLAST hits with high support (posterior probability of 1.00). Despite the fact that more basal branches within the GHF30 clusters are not well resolved, the GHF30 cluster itself forms a monophyletic group with high support.

A BLASTP search with the putative CBM resulted in fewer hits, all from bacteria (Table 1). An alignment is shown in Fig. 5. Only the first two hits (both xylanases from *A. punctata)* have a significant match in CDD and are classified as CBM6 (*E*-values = 1e−15 and 7e−10). The other BLAST hits have no matching domains in CDD, although some are classified in different CBM groups by the CAZy classification (Table 1). A HMMer search was performed with profiles for different CBMs against the different proteins retained by the BLAST search. HMM profiles for which a significant hit was found (positive bit score) are indicated in Table 1. The closest homologues, from *A. punctata*, have been assigned to CBM35 according to CAZy. Nevertheless, some homologues belong to CBM13 and CBM22, whereas others have not been assigned to a CBM family at all. A HMMer search with different CBM profiles resulted in even more confusion, as some CBMs showed positive bit scores to different CBM families, for example CBM35 members

**Fig. 4** Phylogenetic tree including the closest homologues of the catalytic domain of Rs-XYL1. Ten glycosyl hydrolase family 5 (GHF5) enzymes were included and three GHF10 enzymes were chosen as outgroup. The tree was deduced by Bayesian analysis with $10^6$ generations with a sample frequency of 100. Posterior probabilities are shown on the branches. The GHF5 cluster includes true GHF5 enzymes selected from the PFAM seed alignment for GHF5. The lower cluster, indicated as Rs-XYL1 top BLAST hits, includes all BLAST hits from a BLASTP search with the catalytic domain of Rs-XYL1 as query with *E*-values between 1e−73 and 1e−22. The other sequences within the GHF30 cluster include BLASTP hits with *E*-values between 1e−14 and 1e−4. Fungal and nematode sequences are indicated; all other sequences are bacterial. Stars indicate enzymes that are classified as GHF5 according to the CAZy classification.

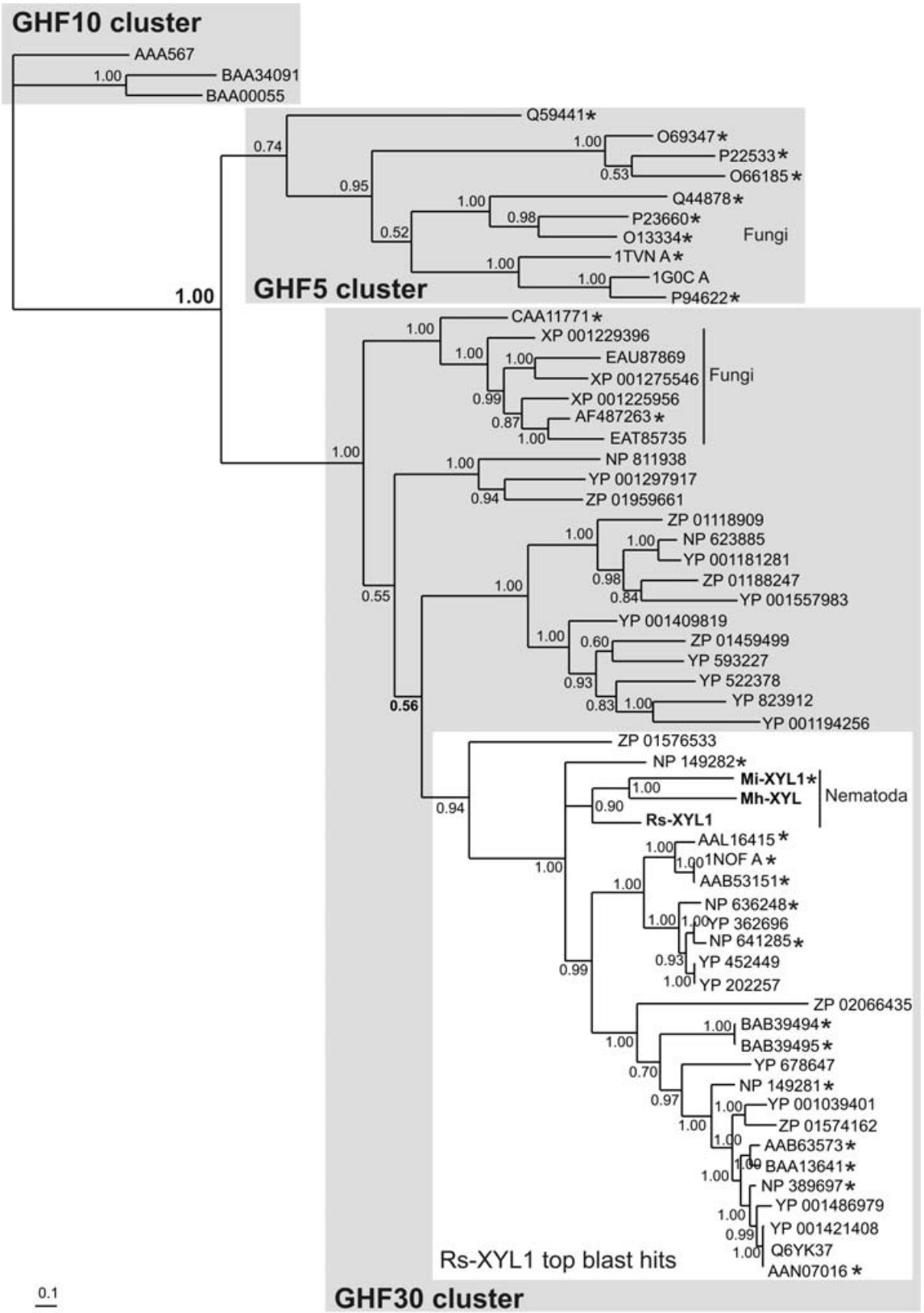

**Table 1** Closest homologues to the Rs-XYL1 carbohydrate-binding module (CBM), as identified by BLASTP ($E < 1e{-}4$). The species name, accession number and description of the protein are given. The CAZy classification (http://www.cazy.org) and Hidden Markov Model (HMM) profiles that resulted in a significant hit (positive bit score) are indicated.

| Species | ACC | Description | BLASTP *E*-value | CAZy | HMM search |
|---|---|---|---|---|---|
| *Radopholus similis* | EU190885 | Endo-1,4-β-xylanase | — | — | — |
| *Aeromonas punctata* | AAB63573 | Xylanase D | 2.00e−14 | CBM35 | CBM6, CBM35 |
| *Aeromonas punctata* | BAA13641 | Endo-xylanase | 9.00e−14 | CBM35 | CBM6, CBM35 |
| *Clostridium cellulolyticum* | ZP_01574162 | Carbohydrate-binding family 6 | 2.00e−12 | — | — |
| *Bacillus subtilis* | NP_389697 | Hypothetical protein | 4.00e−11 | — | — |
| *Bacillus subtilis* | Q6YK37 | Glucuronoxylanase xynC precursor | 5.00e−11 | — | — |
| *Bacillus amyloliquefaciens* | YP_001421408 | YnfF | 7.00e−11 | — | — |
| *Clostridium acetobutylicum* | NP_149281 | Possible xylan degradation enzyme | 3.00e−09 | CBM13 | CBM13 |
| *Clostridium acetobutylicum* | NP_149282 | Possible xylan degradation enzyme | 3.00e−08 | CBM13 | CBM13 |
| *Clostridium cellulolyticum* | ZP_01576533 | Cellulosome enzyme, dockerin type I | 8.00e−08 | — | CBM6, CBM35 |
| *Ruminococcus albus* | BAB39494 | xynC | 8.00e−08 | CBM22 | CBM4(9) |
| *Ruminococcus albus* | BAB39495 | Xylanase C | 3.00e−07 | CBM22 | CBM4(9) |
| *Clostridium thermocellum* | YP_001039401 | Carbohydrate-binding family 6 | 5.00e−07 | — | CBM6 |
| *Cytophaga hutchinsonii* | YP_678647 | CHU large protein, candidate xylanase | 7.00e−07 | — | — |
| *Bacillus subtilis* | AAN07016 | YnfF | 2.00e−05 | — | — |

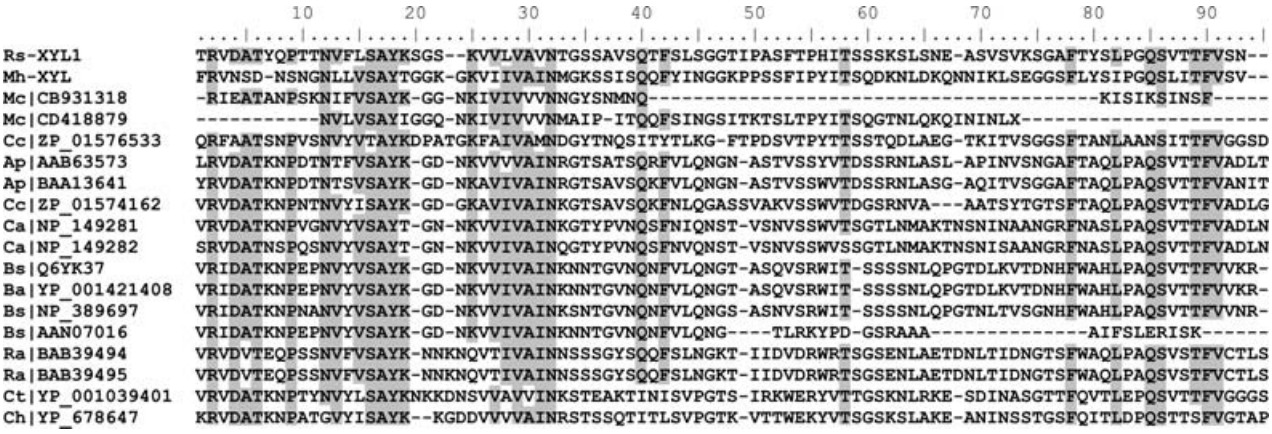


**Fig. 5** Alignment of the carbohydrate binding module of Rs-XYL1 with its closest homologues (BLASTP hits with *E*-value < 1e−4), Mh-XYL and two translated expressed sequence tags (ESTs) from *Meloidogyne chitwoodi*. Ap, *Aeromonas punctata*; Ba, *Bacillus amyloliquefaciens*; Bs, *Bacillus subtilis*; Ca, *Clostridium acetobutylicum*; Cc, *Clostridium cellulolyticum*; Ch, *Cytophaga hutchinsonii*; Ct, *Clostridium thermocellum*; Mc, *Meloidogyne chitwoodi*; Mh, *Meloidogyne hapla*; Ra, *Ruminococcus albus*. The threshold for shading is 75%.

were also recognized as CBM6 (Table 1). None of the HMM profiles matched the putative CBM of Rs-XYL1.

All nematode ESTs were searched for homologues to the endoxylanase domains. The top hits (*E*-value < 1e−20) of the TBLASTN search with the catalytic domain were all ESTs derived from the genus *Meloidogyne*: *M. chitwoodi* (CB931318, CD418879), *M. arenaria* (CF357210, CF357155) and *M. javanica* (CF350477, CF350376). Other hits (*E*-value < 1e−4) were from *Globodera pallida* (BM415401, CV578872) and *Caenorhabditis elegans* (AU208008, BJ762920, CB388002). The latter show less similarity and are most probably not endoxylanases, but other glycosyl hydrolases and glucosylceramidases, probably involved in glycan degradation and sphingolipid metabolism (EC 3.2.1.45, BRENDA database) (Barthelmes *et al.*, 2007). A TBLASTN search with the CBM resulted in only two hits (*E*-value < 1e−3), both from *M. chitwoodi* (CB931318, CD418879).

## Temporal and spatial expression of *Rs-xyl1*

The expression level of *Rs-xyl1* was compared for different life stages by semi-quantitative reverse transcriptase-polymerase chain reaction (RT-PCR) (Fig. 6). In developing embryos and juveniles, no expression of *Rs-xyl1* was detected, whereas males and females revealed approximately similar expression levels. To

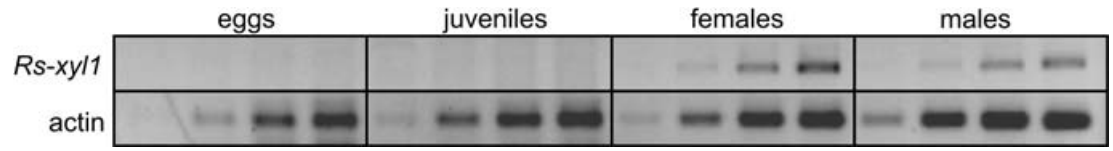


**Fig. 6** Expression of *Rs-xyl1* and actin in developing embryos (27, 30, 33 and 36 cycles), juveniles (30, 33, 36 and 39 cycles), females (21, 24, 27 and 30 cycles) and males (24, 27, 30 and 33 cycles) of *Radopholus similis*.

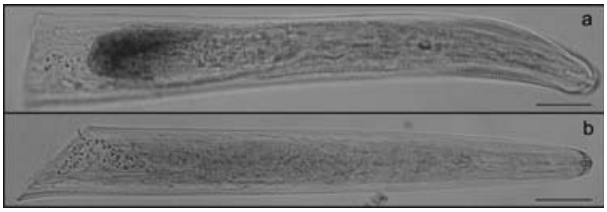


**Fig. 7** Whole-mount *in situ* hybridization on *Radopholus similis*: (a) *Rs-xyl1* antisense probe; (b) *Rs-xyl1* sense probe. Scale bar, 20 μm.

localize the transcripts, a whole-mount *in situ* hybridization was carried out (Fig. 7). The antisense probe showed clear staining in the gland cell area. The sense probe used as negative control showed no staining.

### Silencing of *Rs-xyl1* by RNA interference (RNAi) and infection tests

Batches of freshly harvested nematodes were soaked in double-stranded RNA (dsRNA) against green fluorescent protein (dsgfp), water or dsRNA against *Rs-xyl1* (either targeting the catalytic domain or the putative CBM). After soaking, the expression level of *Rs-xyl1* was checked by semi-quantitative RT-PCR. Actin was amplified to approximately the same level in all samples.

In one of the three experiments, no differences in the expression level of *Rs-xyl1* could be detected between the different treatments. The corresponding infection experiment showed no significant differences in infection of the soaked nematodes compared with the controls.

In the other two experiments, *Rs-xyl1* showed a lower expression level in the nematodes soaked in dsRNA targeted to the CBM when compared with the controls (dsgfp and water). No silencing of *Rs-xyl1* could be detected in nematodes soaked in dsRNA targeted to the catalytic domain. Both corresponding infection experiments showed a significant ($P < 0.01$) decrease in the infection (53% and 66%) of nematodes soaked in dsRNA targeted against the CBM of *Rs-xyl1* compared with nematodes soaked in dsgfp or water. Interestingly, nematodes soaked in dsRNA targeting the catalytic domain of *Rs-xyl1* appeared to show a slight decrease in infection, but this was not significantly different from the controls. The data of one of these experiments are graphically represented in Fig. 8.

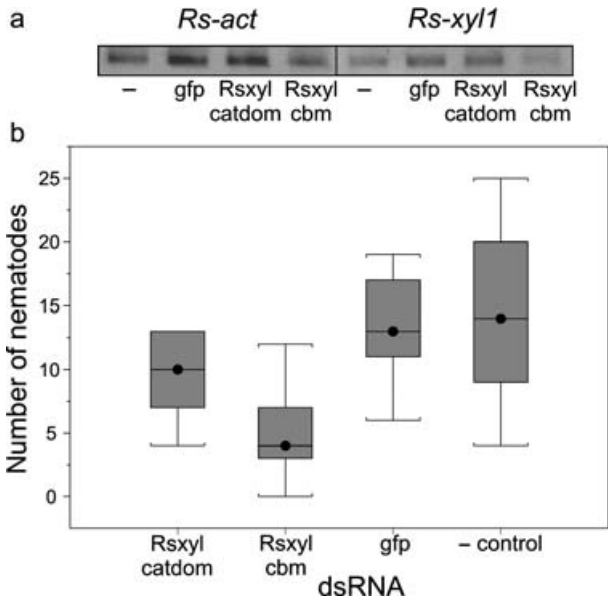


**Fig. 8** Silencing of *Rs-xyl1*. (a) Semi-quantitative reverse transcriptase-polymerase chain reaction (RT-PCR) with primers against actin (30 cycles) and *Rs-xyl1* (36 cycles) on RNA extracted from nematodes soaked in double-stranded RNA (dsRNA) against *Rs-xyl1* located in the catalytic domain (Rsxyl-catdom), dsRNA against *Rs-xyl1* located in the putative carbohydrate-binding module (CBM) (Rsxyl-cbm), double-stranded RNA against green fluorescent protein (gfp) and water (– control). (b) Box-plot of the number of *Radopholus similis* in the root tissue per plate 10 days after inoculation with soaked nematodes. Eleven plants were used for each treatment. The length of the vertical bar denotes the interquartile range, the middle bar represents the median, and the upper and lower horizontal bars denote the upper and lower quartiles, respectively.

## DISCUSSION

During the last decade, different endogenous cell wall-degrading enzymes have been identified in plant-parasitic nematodes. These enzymes facilitate the penetration and migration of the nematode through the rigid plant tissue by softening the plant cell walls. Although xylan is an important component of this cell wall, endoxylanases have only been described for the sedentary nematode species *Meloidogyne* (Mitreva-Dautova *et al.*, 2006).

In this study, we report the identification and characterization of the first putative endoxylanase (*Rs-xyl1*) of a migratory nematode, *R. similis*. The overall GC content of the coding sequence (61%) is higher than the average value (54%) (Jacob *et al.*, 2008), and

 

is a result of the high GC3 (85% rather than 65%). This high GC3 content was also observed for the secreted endo-1,4-β-glucanases of this species (Haegeman *et al.*, 2008). The gene contains three short introns (less than 50 bp). Interestingly, a putative endoxylanase found in the genome sequence of *M. hapla* (contig 2188, http://www.hapla.org) revealed three predicted introns at the same position as the introns of *Rs-xyl1*, and two isolated genomic endoxylanase sequences of the root-knot nematode *M. incognita* showed a single intron at the same position as the second intron of *Rs-xyl1*. This indicates that these introns were probably already present in the common ancestor xylanase gene of these species. The phylogenetic analysis confirmed the close phylogenetic relationship of the nematode endoxylanases. The isolated genomic sequences of *M. incognita* xylanases (*Mi-xyl2*, *Mi-xyl3*) are very similar to the previously described xylanase *Mi-xyl1* (Mitreva-Dautova *et al.*, 2006). If these genes are not allelic variants, they probably originated from the same ancestral gene through duplications.

The main difference between the putative endoxylanase of *R. similis* and the previously identified endoxylanase of *M. incognita* is the presence of a putative CBM in Rs-XYL1 (Fig. 2). This putative CBM was also present in the genomic sequence found in the *M. hapla* genome, and BLAST searches against the *M. incognita* genome revealed that it is probably also associated with the six identified endoxylanases in the genome (Abad *et al.*, 2008). Three-dimensional modelling of the protein revealed that the CBM consists of eight β-strands, and that the first β-strand at the N-terminal end of the mature protein contributes to the β-sandwich, as is the case for the *Erwinia chrysanthemi* xylanase 1NOF. The presence of a putative CBM in Rs-XYL1 is not surprising, because most bacterial endoxylanases are also associated with a CBM. Although difficult to prove, it is a possibility that nematode endoxylanases have originated through the horizontal gene transfer of a bacterial endoxylanase, as also suggested for nematode endoglucanases (Keen and Roberts, 1998). In this view, it is more likely to find an endoxylanase with a CBM in nematodes. The putative endoxylanase found in the genome of *M. hapla* also includes a putative CBM. A search through the nematode ESTs with the putative CBM of Rs-XYL1 resulted in two hits from *M. chitwoodi*. These tags were also retained by a BLASTX search using the catalytic domain as query. Therefore, it seems that other nematode endoxylanases possibly also have a CBM. Endoxylanases without a CBM, such as Mi-XYL1, could have lost this domain during evolution.

The amino acid sequence of the catalytic domain showed significant similarity to the *M. incognita* xylanase Mi-XYL1 as well as to different bacterial endoxylanases of GHF5 and GHF30. As the closest homologues of the protein have been assigned to GHF5, it is tempting to classify Rs-XYL1 in the same subclass. However, it should be noted that the GHF5 signature, which consists of a consensus sequence motif of 10 amino acids, shows three mismatches in both Rs-XYL1 and Mi-XYL1, and two mismatches in Mh-XYL and most bacterial endoxylanases that appeared as best hits in our BLAST search, questioning their classification as GHF5 proteins. Moreover, none of these proteins shows significant similarity to the HMM GHF5 profile, whereas all proteins (except for Mi-XYL1) have a significant match to the GHF30 profile. The fact that Mi-XYL1 is not recognized by the HMM profile of GHF30 is probably a result of the limited seed alignment from only three sequences on which the profile has been based. Keen *et al.* (1996) suggested that this group of endoxylanases should be classified in an intermediate class between GHF5 and GHF30. Unfortunately, this idea never caught on, and the enzymes were later assigned to GHF5, resulting in an inconsistent classification. In the phylogenetic analysis of this study, we were able to show that Rs-XYL1 and related endoxylanases form a monophyletic cluster with other GHF30 enzymes. We can conclude that the endoxylanase homologues are a subclass of GHF30, rather than GHF5, and that previous classifications of some of these enzymes into GHF5 are incorrect.

In analogy with the difficulties in classifying the catalytic domain, it is not clear to which family the CBM domain belongs. Similarity was found to proteins belonging to different CBM families, and a number of homologues are not properly classified themselves. This implies that the CBM classification needs to be revised for some families.

The expression of *Rs-xyl1* could only be demonstrated in the adult stages of *R. similis* and not in eggs or juveniles. This suggests that the putative endoxylanase only plays a role in later life stages, which is not what is expected, as both juvenile and adult stages migrate and feed within the root tissue. Although adult males of *R. similis* do not feed, the expression level of *Rs-xyl1* in males is the same as that in females. This expression pattern differs from the expression of endoglucanases, which show a lower level in males (Haegeman *et al.*, 2008). The expression of *Rs-xyl1* is located in the gland cell area of *R. similis*, as shown by *in situ* hybridization (Fig. 7). The fact that the putative protein sequence contains a signal peptide for secretion, and that the gene is expressed in the gland cell area, suggests that the protein is secreted through the stylet of the nematode. Once released into the plant tissue, the putative endoxylanase can break down xylan present in the plant cell wall. The functional importance of the putative endoxylanase was proven by RNAi and infection experiments. When dsRNA targeted to the putative CBM was applied to nematodes, partial silencing of *Rs-xyl1* occurred, whereas no silencing could be observed when dsRNA was based on the catalytic domain. This difference in silencing effect caused by different target regions in the same gene has also been observed for a pectate lyase of *Heterodera glycines* (Sukno *et al.*, 2007). Moreover, in one of the experiments, no silencing could be detected at all. Therefore, it seems that the silencing effect can vary according to the position of the target sequence of the gene, but also

according to the replication of the experiment itself. When *Rs-xyl1* had a lower expression level after treatment with dsRNA targeted to CBM, a significant decrease in infection of, on average, 60% was detected. In the one experiment in which there was no silencing effect, no significant decrease in infection was observed. This suggests that *Rs-xyl1* indeed plays an important role in the infection process. We observed a slight, but statistically insignificant, decrease in infection with the nematodes were soaked in dsRNA targeted to the catalytic domain but, as we did not see a clear reduction in expression, we cannot draw any conclusions for this construct. Nevertheless, this experiment proves that the RNAi technique, so far almost exclusively studied in sedentary nematodes (Lilley *et al.*, 2007), can be successful in reducing the infection of migratory nematodes as well. In one other migratory nematode, *B. xylophilus*, it has been shown recently that RNAi can effectively reduce gene expression and cause lethality, but effects on plant parasitism were not studied (Park *et al.*, 2008).

A search for other xylanase homologues in nematode ESTs did not reveal any new candidate xylanase genes. Homologues were found in *M. chitwoodi*, *M. arenaria* and *M. javanica*, as also described by Mitreva-Dautova *et al.* (2006). Despite the available EST sequence information, endo-1,4-β-xylanases have not been found extensively, in contrast with, for example, endoglucanases. Nevertheless, in this study, we have shown that a putative endoxylanase of a migratory nematode, *R. similis*, is important in the infection process.

## EXPERIMENTAL PROCEDURES

### Nematode cultures, DNA extraction, RNA extraction and cDNA synthesis

*Radopholus similis* was cultured on carrot discs in small Petri dishes, as described by Jacob *et al.* (2007). Mixed stages were collected by rinsing the Petri dishes with distilled water 6–8 weeks after inoculation. *Meloidogyne incognita* was cultured on the roots of pea (*Pisum sativa*). The seeds were sterilized by soaking them for 30 min in sterile distilled water, for 5 min in 100% ethanol, for 15 min in 5% NaOCl and 1% Tween-20, and afterwards washing them five times in sterile water. The sterile seeds were germinated on KNOP (2.4 mM $KNO_3$, 160 μM $MgSO_4.7H_2O$, 1.0 mM $Ca(NO_3)_2.4H_2O$, 400 μM $KH_2PO_4$, 7.0 μM EDTA ferric sodium salt, 0.25 μM $ZnSO_4.7H_2O$, 0.058 μM $CuSO_4.5H_2O$, 0.043 μM $Na_2MoO_4.2H_2O$, 0.025 μM $CoCl_2.6H_2O$, 8.6 μM $H_3BO_3$, 2.9 μM $MnCl_2.4H_2O$, 6.8 μM NaCl, 0.56 mM myo-inositol, 8.1 μM nicotinic acid, 4.9 μM pyridoxine HCl, 30 μM thiamine HCl, 1% sucrose, 0.8% agar; adjusted to pH 6.4) medium and grown at 21 °C. After 2–3 weeks, the root tips were infected with nematodes of the J2 stage and the plants were incubated at 28 °C. About 7 weeks after inoculation, galls with egg masses were dissected and allowed to hatch in sieves in sterile water at 28 °C.

Genomic DNA was isolated from approximately 5000 individuals, as described by Bolla *et al.* (1988). RNA was extracted with TRIzol (Invitrogen, Carlsbad, CA, USA), according to the manufacturer's instructions. RNA was treated with DNAse (Fermentas, St. Leon-Rot, Germany) to avoid DNA contamination. First-strand cDNA was synthesized from 1 μg of RNA in the presence of 4 mM deoxynucleoside triphosphates (dNTPs), 0.5 μM oligodT primer, 10 mM dithiothreitol (DTT), 50 mM Tris-HCl (pH 8.3), 75 mM KCl, 3 mM $MgCl_2$ and 200 U Superscript II Reverse Transcriptase (Invitrogen). The reaction mixture was incubated for 2 h at 42 °C. For RT-PCR analysis, RNA was extracted from approximately 100 individuals, and cDNA was obtained and amplified with the SMART PCR cDNA synthesis kit (Clontech, Palo Alto, CA, USA).

### Activity assay and cloning of *Rs-xyl1*

Approximately 10 000 freshly harvested nematodes were crushed in 0.5 mL TE buffer [10 mM Tris-HCl, 1.0 mM ethylenediaminetetraacetic acid (EDTA), pH 8.0] to which 0.5 mM DTT was added. The sample was centrifuged for 5 min at 2000 ***g*** in a table-top centrifuge, and 2 μL of the supernatant was loaded onto a 1.5% agar plate containing 0.5% xylan from beechwood (Sigma, St. Louis, MO, USA). After overnight incubation at 37 °C, the plate was stained for 15 min with 0.1% Congo Red and subsequently washed for 15 min with 1.0 M NaCl. Water rinsed from uninfected carrot discs was used as a negative control.

Primers Rs-xyl-F and Rs-xyl-R (Table 2) constructed on EST EY194441 were used in PCR. The reaction mixture contained 150 ng of DNA as template, 0.5 μM of each primer, 4 mM dNTPs, 10 mM DTT, 50 mM Tris-HCl (pH 8.3), 75 mM KCl and 1 U of *Taq* DNA polymerase (Invitrogen). The PCR conditions were as follows: 35 cycles of 1 min at 94 °C, 1 min at 54 °C and 1 min at 72 °C. PCR products were loaded onto a 0.5 × TAE 1.5% agarose gel, and the fragments of interest were gel excised and purified with the QIAquick gel extraction kit (Qiagen, Hilden, Germany). The purified fragments were ligated into pGEM-T (Promega, Madison, WI, USA), and the ligation mixture was used for transformation into *Escherichia coli* DH5α cells. Transformed cells were selected on Luria–Bertani (LB) agar plates supplemented with 100 μg/mL carbenicillin. Positive colonies were identified by a colony PCR under standard conditions using SP6 and T7 primers (Table 2). Plasmids were extracted using the Nucleobond AX kit (Machery-Nagel, Düren, Germany), and the inserts were sequenced at the VIB Genetic Service Facility (VIB-GSF, Antwerp, Belgium). Based on the sequence obtained, primers were developed for upstream and downstream walking using the Genome Walker Universal Kit (Clontech), according to the manufacturer's instructions, in two successive PCRs. The primers used for upstream walking were Rs-xyl-up1 and Rs-xyl-up2; those for downstream

 

**Table 2** Primers used for cloning, *in situ* hybridization, reverse transcriptase-polymerase chain reaction (RT-PCR) and RNA interference (RNAi) of *Radopholus similis* and *Meloidogyne incognita* endoxylanases (Invitrogen).

| Primer | Sequence |
|---|---|
| Rs-xyl-F | AAGGGCAAGCAGGTGTGGATG |
| Rs-xyl-R | TGATGCTCAGTTGGAGACGAAG |
| Rs-xyl-up1 | CATCATACTGGTCCAGTCGAAGC |
| Rs-xyl-up2 | TAGTGCTCCGTCATCCACACCTGC |
| Rs-xyl-down1 | AAGAGCGGCGCATTCACCTACTC |
| Rs-xyl-down2 | CTTCGTCTCCAACTGAGCATCA |
| Rs-xyl-start | ATGTTCGCCCTTCTCGTTCCTG |
| Rs-xyl-stop | TCAGTTGGAGACGAAGGTGGTGACG |
| ACT-F | GAAAGAGGGCCGGAAGAG |
| ACT-R | AGATCGTCCGCGACATAAAG |
| Mi-xyl-F | TTTGGTGGTTCTAGTGCTTGG |
| Mi-xyl-R | TGTTGTTGGATTTTCAGTAGCA |
| SP6 | ATTTAGGTGACACTATAGAATACTCAAGC |
| T7 | TAATACGACTCACTATAGGGCGAATTGG |
| OligodT | TTTTTTTTTTTTTTTTTTTTTTTTVN |
| Rs-xyl-catdomF | CCGCCTCGATGAAGTCCAACAAC |
| Rs-xyl-catdomR | GGGTCAGTGAGTGCCTTGTTG |
| Rs-xyl-CBMF | CCAACGTGTTTCTGAGCGCCTAC |
| Rs-xyl-CBMR | TCAGTTGGAGACGAAGGTGGTGAC |
| GFP-F | ATCCGCCACAACATCGAGG |
| GFP-R | TTGTACAGCTCGTCCATGC |
| Rs-xyl-F2 | GGTATGCAGTTGGCTCTGGT |
| Rs-xyl-R2 | GACACAACGCTGACAGTTGG |

walking were Rs-xyl-down1 and Rs-xyl-down2 (Table 2). The fragments of interest were cloned and sequenced as described above. An additional primer set (Rs-xyl-start and Rs-xyl-stop, Table 2) was developed to amplify the full-length coding sequence of the putative endoxylanase from a cDNA pool. The resulting cDNA fragment was cloned in pGEM-T and sequenced as described above.

Primers Mi-xyl-F and Mi-xyl-R (Table 2) were developed based on the endoxylanase coding sequence of *M. incognita* (AF224342). These primers were used in a standard PCR reaction on DNA of *M. incognita*, and the resulting fragments were cloned and sequenced as described above.

## Sequence analysis

To identify introns, cDNA and genomic sequences were compared with ClustalW (Thompson *et al.*, 1994) using default parameters. The overall GC content and the GC content of the first, second and third positions of the codons (GC1, GC2 and GC3) were calculated by an in-house Perl program. The cDNA sequence was translated to protein using the emboss program 'Transeq' (Rice *et al.*, 2000). The molecular weight of the putative protein was calculated with the 'pI/Mw' tool on the ExPASy Proteomics server (Gasteiger *et al.*, 2003). The presence of signal peptides was predicted with SignalP 3.0 configured for eukaryotic sequences (Bendtsen *et al.*, 2004), and *N*-glycosylation sites were predicted by NetNGlyc (http://www.cbs.dtu.dk/services/NetNGlyc/). Tertiary structure predictions were performed in swiss-model (Guex and Peitsch, 1997) using the first approach mode and the crystal structure of a xylanase of *Erwinia chrysanthemi* (PDB entry 1NOF) (Larson *et al.*, 2003) as template (*E*-value = 2.0e−81). The PDB coordinates obtained were visualized using Deepview spdbv 3.7 (Swiss-PdbViewer) and rendered with POV-Ray version 3.6. Because of a lack of similarity to 1NOF, the first 12 amino acids of the mature protein were not modelled by the first approach mode, and these were manually fitted into the model. To identify possible domains in the putative protein sequence of the endoxylanase, a domain search was performed with InterProScan (Zdobnov and Apweiler, 2001). A blastp search with default settings was performed with the catalytic domain and the putative CBM (September 2008). Sequences of the closest homologues were retrieved from GenBank and a protein alignment was constructed with the ClustalW algorithm (Thompson *et al.*, 1994) in BioEdit 7.0.5.3 (Hall, 1999). A local HMM search was performed with HMMER 2.3.2 (http://hmmer.janelia.org) against the closest homologues of the Rs-XYL1 catalytic domain with profiles from GHF5 and GHF30 downloaded from the PFAM website (Finn *et al.*, 2006). The CAZy website (http://www.cazy.org) was searched to find to which CBMs the closest homologues of the Rs-XYL1 CBM could be assigned. A local HMMer search was performed against the closest homologues of the CBM with the following CBM profiles downloaded from the PFAM website: CBM4_9 (PF02018), CBM6 (PF03422), CBM13 (PF00652). The HMM profile of CBM35 was constructed locally from raw sequences. To identify homologous sequences in other nematode species, tblastn searches with the catalytic domain and the CBM were performed against all nematode ESTs. The nematode genome of *M. hapla* was searched for putative endoxylanases by tblastn with Rs-XYL1 as query on the website of the genome project (http://www.hapla.org) (Opperman *et al.*, 2008).

A phylogenetic tree was constructed including the 100 best hits from a blastp search with the catalytic domain. Ten protein sequences which belong to the PFAM seed alignment from GHF5 were selected, as diverse as possible (both mannanases and endoglucanases from bacteria and fungi). Three protein sequences belonging to GHF10 were chosen as outgroup. The phylogenetic analysis was performed by Bayesian statistics using the WAG-model in MrBayes 3.1.2 (Ronquist and Huelsenbeck, 2003), with $10^6$ generations and a sample frequency of 100. The first 2500 generations were considered as burn-in. The resulting tree was visualized in TreeView 1.6.6 (Page, 1996).

## Spatial and temporal expression of *Rs-xyl1*

An *in situ* hybridization was performed according to Jacob *et al.* (2007). Probes were generated by a linear PCR with a single

primer (Rs-xyl-F, sense probe; Rs-xyl-R, antisense probe) in the presence of digoxigenin (DIG)-labelled oligonucleotides (Roche, Mannheim, Germany). As template for the probe generating PCR, the product of a first PCR was used. This PCR was performed on a plasmid containing the corresponding xylanase cDNA fragment with primers Rs-xyl-F and Rs-xyl-R. All PCRs were carried out as described above.

A semi-quantitative RT-PCR on different life stages was performed according to Haegeman *et al.* (2008). The primers used were Rs-xyl-F and Rs-xyl-R and, as a positive control, actin (EU000540) was amplified using the primers ACT-F and ACT-R (Table 2).

### Generation of dsRNA, soaking, infection tests and semi-quantitative RT-PCR

Two different regions of *Rs-xyl1* were selected as target for silencing by RNAi, one in the catalytic domain (286 bp) and one in the putative CBM (242 bp) of *Rs-xyl1*. These regions were amplified by PCR under standard conditions with the T7 promoter sequence incorporated at the 5′ end of either the sense or antisense strand. Primers used for the first region were Rs-xyl-catdomF and Rs-xyl-catdomR, and primers for the second region were Rs-xyl-CBMF and Rs-xyl-CBMR. dsRNA against *gfp* was prepared from a *gfp*-containing construct using primers GFP-F and GFP-R. PCR products were employed as templates for *in vitro* transcription reactions using a Megascript RNAi kit (Ambion, Huntingdon, Cambridgeshire, UK). The dsRNA was quantified spectrophotometrically. A few thousand nematodes of mixed stages were soaked in 50 mM octopamine, 3 mM spermidine, 0.05% gelatin and 0.5 mg/mL dsRNA for 24 h at room temperature on a rotator in the dark. As an extra negative control, nematodes were incubated in the same solution, but without dsRNA. After soaking, the nematodes were sterilized for 1 h in 0.33% hospital antiseptic concentrate (HAC) on a rotator at room temperature and subsequently washed three times with sterile water. Seedlings from *Medicago truncatula* L. var. Jemalong were grown in six-well plates on modified Strullu Romand medium (Elsen *et al.*, 2000). After 3 weeks, the seedlings were infected with 50 sterilized soaked nematodes per plant, 11 plants for each condition. The plants were grown at 22 °C and light/dark cycles of 16 h/8 h. Ten days later, the roots were stained with acid fuchsin (Byrd *et al.*, 1983), destained using acidified glycerol and the nematodes inside the roots were counted using a dissection microscope. The results were statistically analysed in S-PLUS 7.0. Normality was checked with the Kolmogorov–Smirnov test, homoscedasticity with a modified Levene test and analysis of variance (ANOVA) was performed using the Tukey method. The soaking and infection tests were repeated three times. For semi-quantitative RT-PCR, approximately 5000 soaked nematodes were used. RNA extraction and cDNA synthesis were performed as described above. The primers ACT-F and ACT-R were used to amplify actin, whereas Rs-xyl-F2 and Rs-xyl-R2 were used to amplify *Rs-xyl1*. The amount of cDNA added as template and the number of PCR cycles were optimized for each gene product to detect the exponential phase of the reaction. The resulting products were separated on a 0.5 × TAE gel.

## ACKNOWLEDGEMENTS

This research was supported by a grant from Ghent University (GOA 01G00805) and a grant to Annelies Haegeman from the Institute for the Promotion of Innovation through Science and Technology in Flanders (IWT-Vlaanderen). Bartel Vanholme is a postdoctoral researcher at Ghent University (BOF).

## REFERENCES

**Abad, P., Gouzy, J., Aury, J.M., Castagnone-Sereno, P., Danchi, E.G.J., Deleury, E., Perfus-Barbeoch, L., Anthouard, V., Artiguenave, F., Blok, V.C., Caillaud, M.C., Coutinho, P.M., Dasilva, C., De Luca, F., Deau, F., Esquibet, M., Flutre, T., Goldstone, J.V., Hamamouch, N., Hewezi, T., Jaillon, O., Jubin, C., Leonetti, P., Magliano, M., Maier, T.R., Markov, G.V., McVeigh, P., Pesole, G., Poulain, J., Robinson-Rechavi, M., Sallet, E., Segurens, B., Steinbach, D., Tytgat, T., Ugarte, E., van Ghelder, C., Veronico, P., Baum, T.J., Blaxter, M., Bleve-Zacheo, T., Davis, E.L., Ewbank, J.J., Favery, B., Grenier, E., Henrissat, B., Jones, J.T., Laudet, V., Maule, A.G., Quesneville, H., Rosso, M.N., Schiex, T., Smant, G., Weissenbach, J. and Wincker, P.** (2008) Genome sequence of the metazoan plant-parasitic nematode *Meloidogyne incognita*. *Nat. Biotechnol.* **26**, 909–915.

**Barthelmes, J., Ebeling, C., Chang, A., Schomburg, I. and Schomburg, D.** (2007) BRENDA, AMENDA and FRENDA: the enzyme information system in 2007. *Nucleic Acids Res.* **35**, D511–D514.

**Bendtsen, J.D., Nielsen, H., von Heijne, G. and Brunak, S.** (2004) Improved prediction of signal peptides: SignalP 3.0. *J. Mol. Biol.* **340**, 783–795.

**Blumenthal, T. and Steward, K.** (1997) RNA processing and gene structure. In: *C. elegans II* (Riddle, D.L., Blumenthal, T., Meyer, B.J. and Priess, J.R., eds), pp. 117–146. New York: Cold Spring Harbor Laboratory Press.

**Bolla, R.I., Weaver, C. and Winter, R.E.K.** (1988) Genomic differences among pathotypes of *Bursaphelenchus xylophilus*. *J. Nematol.* **20**, 309–316.

**Brennan, Y., Callen, W.N., Christoffersen, L., Dupree, P., Goubet, F., Healey, S., Hernandez, M., Keller, M., Li, K., Palackal, N., Sittenfeld, A., Tamayo, G., Wells, S., Hazlewood, G.P., Mathur, E.J., Short, J.M., Robertson, D.E. and Steer, B.A.** (2004) Unusual microbial xylanases from insect guts. *Appl. Environ. Microbiol.* **70**, 3609–3617.

**Byrd, D.W., Kirkpatrick, T. and Barker, K.R.** (1983) An improved technique for clearing and staining plant-tissues for detection of nematodes. *J. Nematol.* **15**, 142–143.

**Collins, T., Gerday, C. and Feller, G.** (2005) Xylanases, xylanase families and extremophilic xylanases. *FEMS Microbiol. Rev.* **29**, 3–23.

**Coutinho, P.M. and Henrissat, B.** (1999) Carbohydrate-active enzymes: an integrated database approach. In: *Recent Advances in Carbohydrate*

 

*Bioengineering* (Gilbert, H.J., Davies, G., Henrissat, B. and Svensson, B., eds), pp. 3–12. Cambridge: The Royal Society of Chemistry.

**de Boer, J.M., McDermott, J.P., Davis, E.L., Hussey, R.S., Popeijus, H., Smant, G. and Baum, T.J.** (2002) Cloning of a putative pectate lyase gene expressed in the subventral esophageal glands of *Heterodera glycines*. *J. Nematol.* **34**, 9–11.

**Doyle, E.A. and Lambert, K.N.** (2002) Cloning and characterization of an esophageal-gland-specific pectate lyase from the root-knot nematode *Meloidogyne javanica*. *Mol. Plant–Microbe Interact.* **15**, 549–556.

**Duncan, L.W. and Moens, M.** (2006) Migratory endoparasitic nematodes. In: *Plant Nematology* (Perry, R.N. and Moens, M., eds), pp. 123–152. Wallingford: CABI Publishing.

**Elsen, A., Declerck, S. and De Waele, D.** (2000) Reproduction of the burrowing nematode (*Radopholus similis*) on Ri T-DNA transformed carrot roots. *Nematology*, **2**, 247–249.

**Finn, R.D., Mistry, J., Schuster-Bockler, B., Griffiths-Jones, S., Hollich, V., Lassmann, T., Moxon, S., Marshall, M., Khanna, A., Durbin, R., Eddy, S.R., Sonnhammer, E.L.L. and Bateman, A.** (2006) Pfam: clans, web tools and services. *Nucleic Acids Res.* **34**, D247–D251.

**Fogain, R.** (2000) Effect of *Radopholus similis* on plant growth and yield of plantains (*Musa*, AAB). *Nematology*, **2**, 129–133.

**Gasteiger, E., Gattiker, A., Hoogland, C., Ivanyi, I., Appel, R.D. and Bairoch, A.** (2003) ExPASy: the proteomics server for in-depth protein knowledge and analysis. *Nucleic Acids Res.* **31**, 3784–3788.

**Guex, N. and Peitsch, M.C.** (1997) SWISS-MODEL and the Swiss-PdbViewer: An environment for comparative protein modeling. *Electrophoresis*, **18**, 2714–2723.

**Haegeman, A., Jacob, J., Vanholme, B., Kyndt, T. and Gheysen, G.** (2008) A family of GHF5 endo-1,4-beta-glucanases in the migratory plant-parasitic nematode *Radopholus similis*. *Plant Pathol.* **57**, 581–590.

**Hall, T.A.** (1999) BioEdit: A biological sequence alignment editor for Windows 95/98/NT. *Nucleic Acids Symp. Series* **41**, 95–98.

**Henrissat, B. and Bairoch, A.** (1996) Updating the sequence-based classification of glycosyl hydrolases. *Biochem J.* **316**, 695–696.

**Hurlbert, J.C. and Preston, J.F.** (2001) Functional characterization of a novel xylanase from a corn strain of *Erwinia chrysanthemi*. *J. Bacteriol.* **183**, 2093–2100.

**Jacob, J., Vanholme, B., Haegeman, A. and Gheysen, G.** (2007) Four transthyretin-like genes of the migratory plant-parasitic nematode *Radopholus similis*: members of an extensive nematode-specific family. *Gene*, **402**, 9–19.

**Jacob, J., Mitreva, M., Vanholme, B. and Gheysen, G.** (2008) Exploring the transcriptome of the burrowing nematode *Radopholus similis*. *Mol. Genet. Genomics*, **280**, 1–17.

**Jaubert, S., Laffaire, J.B., Abad, P. and Rosso, M.N.** (2002) A polygalacturonase of animal origin isolated from the root-knot nematode *Meloidogyne incognita*. *FEBS Lett.* **522**, 109–112.

**John, F.J.S., Rice, J.D. and Preston, J.F.** (2006) Characterization of XynC from *Bacillus subtilis* subsp. *subtilis* strain 168 and analysis of its role in depolymerization of glucuronoxylan. *J. Bacteriol.* **188**, 8617–8626.

**Keen, N.T. and Roberts, P.A.** (1998) Plant parasitic nematodes: digesting a page from the microbe book. *Proc. Natl. Acad. Sci. USA*, **95**, 4789–4790.

**Keen, N.T., Boyd, C. and Henrissat, B.** (1996) Cloning and characterization of a xylanase gene from corn strains of *Erwinia chrysanthemi*. *Mol. Plant–Microbe Interact.* **9**, 651–657.

**Kikuchi, T., Jones, J.T., Aikawa, T., Kosaka, H. and Ogura, N.** (2004) A family of glycosyl hydrolase family 45 cellulases from the pine wood nematode *Bursaphelenchus xylophilus*. *FEBS Lett.* **572**, 201–205.

**Kikuchi, T., Shibuya, H., Aikawa, T. and Jones, J.T.** (2006) Cloning and characterization of pectate lyases expressed in the esophageal gland of the pine wood nematode *Bursaphelenchus xylophilus*. *Mol. Plant–Microbe Interact.* **19**, 280–287.

**Larson, S.B., Day, J., de la Rosa, A.P.B., Keen, N.T. and McPherson, A.** (2003) First crystallographic structure of a xylanase from glycoside hydrolase family 5: implications for catalysis. *Biochemistry*, **42**, 8411–8422.

**Lilley, C.J., Bakhetia, M., Charlton, W.L. and Urwin, P.E.** (2007) Recent progress in the development of RNA interference for plant parasitic nematodes. *Mol. Plant Pathol.* **8**, 701–711.

**Mitreva-Dautova, M., Roze, E., Overmars, H., de Graaff, L., Schots, A., Helder, J., Goverse, A., Bakker, J. and Smant, G.** (2006) A symbiont-independent endo-1,4-beta-xylanase from the plant-parasitic nematode *Meloidogyne incognita*. *Mol. Plant–Microbe Interact.* **19**, 521–529.

**Opperman, C.H., Bird, D.M., Williamson, V.M., Rokhsar, D.S., Burke, M., Cohn, J., Cromer, J., Diener, S., Gajan, J., Graham, S., Houfek, T.D., Liu, Q., Mitros, T., Schaff, J., Schaffer, R., Scholl, E., Sosinski, B.R., Thomas, V.P. and Windham, E.** (2008) Sequence and genetic map of *Meloidogyne hapla*: a compact nematode genome for plant parasitism. *Proc. Natl. Acad. Sci. USA*, **105**, 14 802–14 807.

**Page, R.D.M.** (1996) TreeView: an application to display phylogenetic trees on personal computers. *Comput. Appl. Biosci.* **12**, 357–358.

**Park, J.E., Lee, K.Y., Lee, S.J., Oh, W.S., Jeong, P.Y., Woo, T., Kim, C.B., Paik, Y.K. and Koo, H.S.** (2008) The efficiency of RNA interference in *Bursaphelenchus xylophilus*. *Mol. Cells*, **26**, 81–86.

**Pearl, F.M.G., Bennett, C.F., Bray, J.E., Harrison, A.P., Martin, N., Shepherd, A., Sillitoe, I., Thornton, J. and Orengo, C.A.** (2003) The CATH database: an extended protein family resource for structural and functional genomics. *Nucleic Acids Res.* **31**, 452–455.

**Rice, P., Longden, I. and Bleasby, A.** (2000) EMBOSS: The European molecular biology open software suite. *Trends Genet.* **16**, 276–277.

**Ronquist, F. and Huelsenbeck, J.P.** (2003) MrBayes 3: Bayesian phylogenetic inference under mixed models. *Bioinformatics*, **19**, 1572–1574.

**Rosso, M.N., Favery, B., Piotte, C., Arthaud, L., de Boer, J.M., Hussey, R.S., Bakker, J., Baum, T.J. and Abad, P.** (1999) Isolation of a cDNA encoding a beta-1,4-endoglucanase in the root-knot nematode *Meloidogyne incognita* and expression analysis during plant parasitism. *Mol. Plant–Microbe Interact.* **12**, 585–591.

**Smant, G., Stokkermans, J.P.W.G., Yan, Y.T., de Boer, J.M., Baum, T.J., Wang, X.H., Hussey, R.S., Gommers, F.J., Henrissat, B., Davis, E.L., Helder, J., Schots, A. and Bakker, J.** (1998) Endogenous cellulases in animals: isolation of beta-1,4-endoglucanase genes from two species of plant-parasitic cyst nematodes. *Proc. Natl. Acad. Sci. USA*, **95**, 4906–4911.

**Subramaniyan, S. and Prema, P.** (2002) Biotechnology of microbial xylanases: enzymology, molecular biology, and application. *Crit. Rev. Biotechnol.* **22**, 33–64.

**Sukno, S.A., McCuiston, J., Wong, M.Y., Wang, X.H., Thon, M.R., Hussey, R., Baum, T. and Davis, E.** (2007) Quantitative detection of double-stranded RNA-mediated gene silencing of parasitism genes in *Heterodera glycines*. *J. Nematol.* **39**, 145–152.

**Suzuki, T., Ibata, K., Hatsu, M., Takamizawa, K. and Kawai, K.** (1997) Cloning and expression of a 58-kDa xylanase VI gene (xynD) of *Aeromonas caviae* ME-1 in *Escherichia coli* which is not categorized as a family F or family G xylanase. *J. Ferment. Bioeng.* **84**, 86–89.

**Thompson, J.D., Higgins, D.G. and Gibson, T.J.** (1994) CLUSTALW – improving the sensitivity of progressive multiple sequence alignment through sequence weighting, position-specific gap penalties and weight matrix choice. *Nucleic Acids Res.* **22**, 4673–4680.

**Trinh, P.Q., Nguyen, C.N., Waeyenberge, L., Subbotin, S.A., Karssen, G. and Moens, M.** (2004) *Radopholus arabocoffeae* spn. (Nematoda: Pratylenchidae), a nematode pathogenic to *Coffea arabica* in Vietnam, and additional data on *R. duriophilas*. *Nematology*, **6**, 681–693.

**Uehara, T., Kushida, A. and Momota, Y.** (2001) PCR-based cloning of two beta-1,4-endoglucanases from the root-lesion nematode *Pratylenchus penetrans*. *Nematology*, **3**, 335–341.

**Vanholme, B., Van Thuyne, W., Vanhouteghem, K., De Meutter, J., Cannoot, B. and Gheysen, G.** (2007) Molecular characterization and functional importance of pectate lyase secreted by the cyst nematode *Heterodera schachtii*. *Mol. Plant Pathol.* **8**, 267–278.

**Zdobnov, E.M. and Apweiler, R.** (2001) InterProScan—an integration platform for the signature-recognition methods in InterPro. *Bioinformatics*, **17**, 847–848.

 